

Enhance the Dynamic Performance of DFIGURE during Voltage Sag and Voltage Swell Using SMES

J. Rajesh¹, Venugopal .N²

¹Student, Department of EEE, Kuppam Engineering College, Kuppam, Andhrapradesh, India

² Professor,HOD, Department of EEE, Kuppam Engineering College, Kuppam, Andhrapradesh, India

Abstract: *One of the most important parameters of the incorporation of wind turbines into present day power frameworks has fundamentally expanded amid the most recent decade. Wind turbines furnished with doubly nourished instigation generators (DFIGURES) have been overwhelming wind power establishment worldwide since 2002. In this paper, superconducting attractive vitality stockpiling (SMES) unit is being utilized to enhance the dynamic execution of a wind vitality change framework outfitted with DFIGURE amid voltage droop at the grid side event. The voltage source converter and HCC control power transfer between the SMES curl and the air conditioner framework, a dc–dc chopper is used and fuzzy logic and adaptive neuro-fuzzy inference system is selected to control its duty cycle (D) with input variables real power created by the DFIGURE and the SMES loop current. The MATLAB/SIMULINK software is used to simulate the wind turbine, the SMES unit, and the model under study. Results are to be analyzed to highlight the improved dynamic performance of wind energy conversion systems in conjunction with the SMES unit under voltage sag and voltage swell conditions.*

Keywords: Doubly fed induction generator (DFIGURE), superconducting magnetic energy system (SMES), adaptive neuro-fuzzy inference system (ANFIS), fuzzy logic, hysteresis current controller, wind energy conversion system (WECS).

1. Introduction

The first generation of wind energy conversion systems (WECS) was the direct connected WECS type. This technology uses a fixed speed turbine to generate power. It dominated renewable energy installations worldwide, comprising up to 70% of all installations in 1995. This technology remained popular until the electronic power revolution that updated the WECS so that they could maximize wind energy capture. This technology is called variable speed WECS, and it can optimally capture wind energy 5% more than the fixed speed WECS option. Furthermore, the variable speed WECS can reduce the impact of transient wind gusts and subsequent fatigue unlike the fixed speed turbines. Variable speed WECS, such as doubly fed induction generator (DFIGURE) was introduced to overcome the weakness of the fixed speed type in capturing maximum wind energy and to contribute reactive power to the grid when required. Compared to full scale variable speed WECS, DFIGURE is very sensitive to grid faults; although The DFIGURES are usually connected far away from the grid. This condition will force the DFIGURE to be disconnected from the system. If the DFIGURE contributes to a large portion of power to the grid, then the financial loss of a disconnection would be uncountable. A failure to discharge and flame through that Happens inside both the framework side converter (GSC) and the rotor-side converter (RSC) of the DFIGURE is incorporated in this proposed framework. Discharge failure is the disappointment of the converter switch to take Over conduction at the modified directing period while fire-through is the disappointment of the converter switch to square amid a planned non-leading period. These interior shortcomings are brought on by different glitches in the control and terminating hardware a mechanical review demonstrates that converter blames because of breakdowns inside the control

circuit speak to around 53.1% while around 37.9% of the converter deficiencies are because of converter force parts.

The utilization of a protected entryway bipolar transistor (IGBT) in both DFIGURES' converters is favored because of its playing point which incorporates high exchanging recurrence in a common scope of 2–20 kHz contrasted and the partner door side road transistor exchanging recurrence which does not surpass 1.0 kHz The impact of these switching faults on the performance of DFIGURE with and without SMES will be investigated and discussed.

2. System Under Study

The system under study shown in Figure.1 consists of six 1.5-MW DFIGURES connected to the ac grid at the PCC. The DFIGURE consists of an induction generator with stator winding connected directly to the grid through a Y/Δ step-up transformer, whereas the rotor winding is connected to a bidirectional back-to-back insulated gate bipolar transistor (IGBT) VSC, as shown in Figure.1.

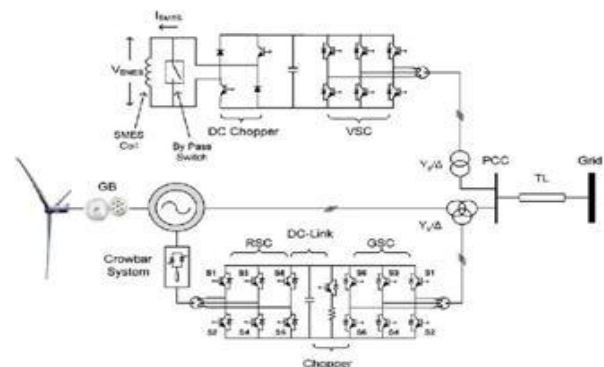


Figure 1: DFIGURE equipped with SMES unit.

The grid that is spoken to by a perfect three-phase voltage wellspring of steady recurrence is connected to the wind turbines via a 30-km transmission line and Δ/Y step-up transformer. The reactive power produced by the wind turbines is regulated at zero MVAR under normal operating conditions. For a normal wind velocity of 15 m/s, which is utilized as a part of this study, the turbine yield force is 1.0 pu, and the generator speed is 1.2 pu. The SMES unit is connected to the 25-kV bus furthermore, is thought to be completely charged at its most extreme limit of 1.0 MJ.

3. SMES Configuration

An SMES system consists of a superconducting coil, a power-conditioning framework. In this framework, a superconducting curl which is kept up at a cryogenic temperature (low temperature underneath 150 deg C) is accused of direct current. The present moving through the curl creates a solid attractive field in which electrical energy is stored as a circulating current; energy can be drawn from put away or conveyed over periods running from a small amount of a second to a few hours. The loop can be arranged as a solenoid or a torrid. The solenoid sort has been utilized broadly because of its straightforwardness and expense viability. Coil inductance or PCS maximum voltage (V_{max}) and current (I_{max}) ratings focus the greatest vitality/control that can be drawn or infused By a SMES curl. A SMES unit with very nearly quick reaction with vitality. It is highly efficiency of the SMES unit in the range of 95%-99%. Other advantages of the SMES unit include very quick response and possibilities for high power applications.

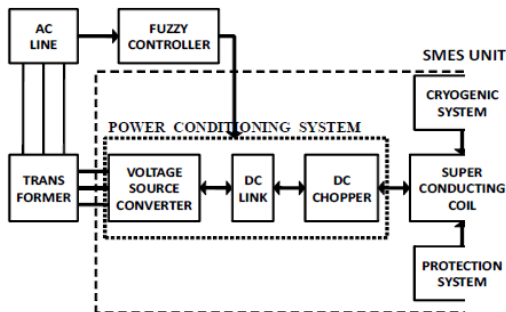


Figure 2: Schematic diagram of a SMES system.

4. SMES Control Scheme

There are two configurations of SMES unit, i.e., current source converter (CSC) and voltage source converter (VSC). If the CSC eliminates fifth and seventh harmonics currents in ac side, but its configuration is in parallel connected use of two 6-pulse CSC, its cost is relatively high. However, the VSC and DC-DC chopper which are connected through a DC shunt capacitor. The VSC is controlled by a hysteresis current controller (HCC) while the DC-DC chopper is controlled by adaptive neuro-fuzzy inference system (ANFIS). It estimates the total cost of the switching devices of the CSC to be 173% of the switching devices and power diodes necessary for equivalent capacity of the VSC and the chopper. Likewise, a VSC has a better self-commutating capability, and it injects lower order harmonic currents into the ac grid than a similar to CSC.

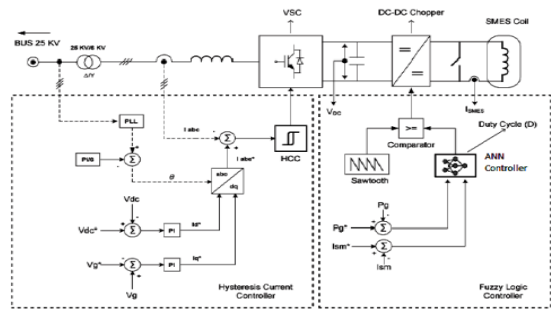


Figure 3: SMES unit configuration and the proposed HCC-ANFIS control scheme.

The use of IGBTs in this conFigureuration is more helpful than GTO since the switching frequency of an IGBT lies on the range of 2–20 kHz, whereas, in case of GTO, the switching frequency cannot exceed 1 kHz. It provides a power electronic interface between the ac power system and the superconducting coil. The control system of the VSC is shown in Figure. 3. The proportional integral (PI) controllers determine the reference d- and q-axis currents by using the difference between the dc link voltage and reference value, and the difference between terminal voltage and reference value, respectively. Its stored energy in the SMES coil can be calculated as

$$E = \frac{1}{2} I_{SMES}^2 L_{SMES}$$

Where E, I_{SMES} , and L_{SMES} are the stored energy, current, and coil inductance of the SMES unit, respectively.

This topology will be only suitable for new WECS installations. Application of the SMES system to micro grids is presented in, where the SMES is used to stabilize the entire micro grid system. The control scheme in this paper comprises only two PI controllers and considers the SMES coil current to take the SMES stored energy capacity into account, along with the DFIGURE generated power as control parameters to determine the direction and level of force trade between the SMES loop and the air conditioner framework. This control system is efficient, simple, and easy to put into practice, as will be modified here.

A. Hysteresis Current Controller (HCC)

The hysteresis current control methods play an important role in power electronic circuits, Nevertheless, due to lack of coordination among individual HCC's of three phases, high switching frequency may happen, and the current error is not strictly limited. The actual current waveform is not only determined by the hysteresis control: depending on operating conditions, the current slope may vary widely and the current peaks may appreciably exceed the limits of the hysteresis band. Figure.3 shows proposed SMES with an auxiliary PLL controller. The PI controller

TABLE I
 RULES OF DUTY CYCLE

Duty Cycle (D)	SMES coil Action
D=0.5	Standby condition
$0 \leq D < 0.5$	Discharging Condition
$0.5 < D \leq 1$	Charging Condition

Determine the reference d- and q-axis currents by using the difference between the dc link voltage V_{dc} and reference value V_{dc}^* , and the difference between terminal (grid) voltage V_g and reference value V_g^* , respectively. The HCC signal is generated for IGBT switching and the HCC compares the three-phase line currents (I_{abc}) with the reference currents (I_{abc}^*), which is dictated by the I_d^* and I_q^* references. The value of I_d^* and I_q^* is converted through Park transformation (dq0-abc) to produce reference current (I_{abc}^*). The dc voltage across the capacitor is kept constant throughout by the converter.

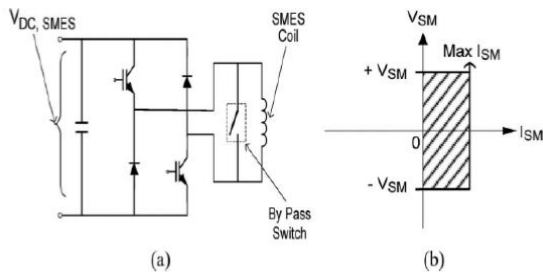


Figure 4: Class-D dc-dc chopper topology with an SMES coil.

B. Adaptive Neuro-Fuzzy Inference System (ANFIS)

The ANFIS has simple data learning technique, that use fuzzy logic to transform given inputs into a desired output through highly interconnected neural network processing elements. Fuzzy logic to controls the duty cycle, and is based on inputs in the form of linguistic variable. These linguistic variables are derived from membership functions. A neural network have shortcoming with their representation of implicit knowledge. The determination of fuzzy rules, inputs, and outputs depends on trial and error, this makes the design of FLS a time consuming task. These drawbacks of NN and FLS can be overcome by the integration of NN technology with a fuzzy logic system. The ANFIS is a fuzzy neural network. The most advantages of using ANFIS are that all its parameters can be trained like a NN within the structure of a FLS.

In the modeling and feedback control of any dynamical system, a controller is a must for the plant as it takes care of all the Disturbances and brings back the system to its original state in a couple of second.

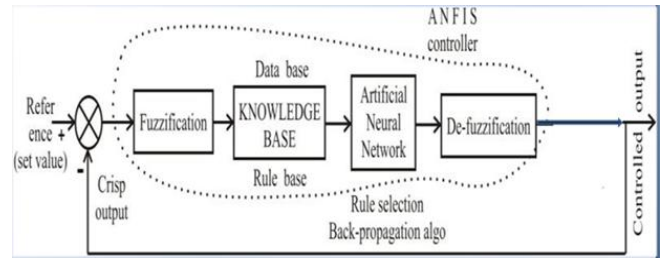


Figure 5: Block diagram of the ANFIS control scheme

To start the design of the controller using the ANFIS scheme, use fuzzification unit changes over the fresh information into phonetic variables, which is given as inputs to the guideline based piece. The arrangements of 49 standards are composed on the premise of past information in the tenet base square. The principle base square is associated with the NN block.

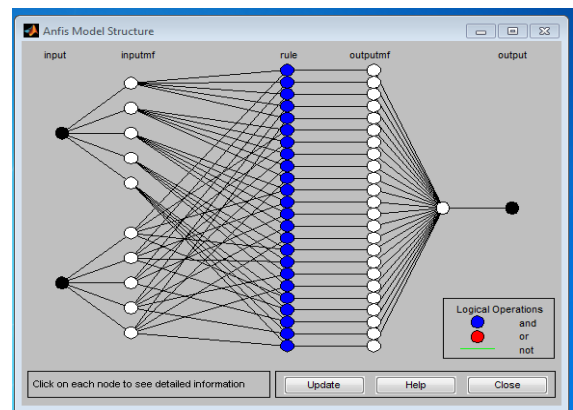


Figure 6: ANFIS model structure

The Back spread calculation is utilized to prepare the neural system to choose the best possible arrangement of principles base once the correct tenets are chosen and terminated the control sign needed to acquire the ideal yields is produced. Its yield of the neural system unit is given as info to the de-fuzzification unit and the semantic variables are changed over once again into the numeric type of information in the fresh frame.

5. Simulation Diagram and Results

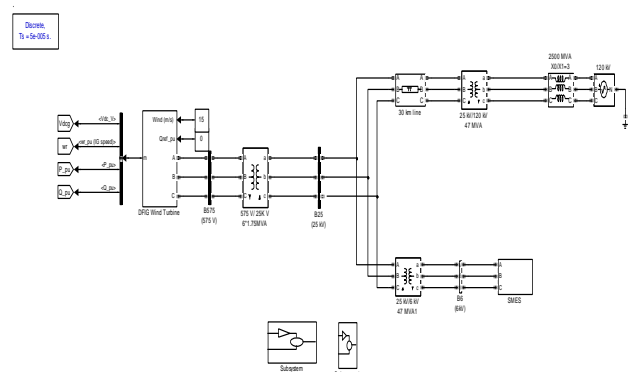


Figure 7: SIMULINK model of DFIGURE connected with SMES and ANFIS

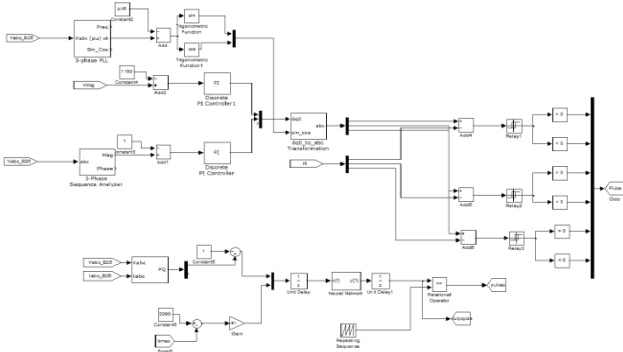


Figure 8: SIMULINK model of control circuit

6. Voltage Sag and Swell Events

A voltage sag and swell depth of 0.5 pu lasting for 0.05s is applied at $t=2s$ at the grid side of the system under study. Without the SMES unit, in this sag event of time duration is 0.8 to 1.4 pu, and swell event of time duration 0.5 to 1.1 pu and it reaches a maximum overshooting of 45% during the freedom of the issue as demonstrated in Figure 9 & 11. As can be seen in Figure 9 & 11, with the SMES unit associated with the framework, the DFIGURE output power will drop to only 0.875 pu. It implies that, with the connection of the SMES unit and during the event of voltage sag, event of time duration 1.2 to 1.5 and sell event of time duration 0.25 to 0.5 and the reactive power support by the DFIGURE is reduced up to 2.51pu, and the steady-state condition is reached faster, compared to the system without SMES. The Figure.13 (a) is the waveform of active power during voltage sag with SMES. Here the power drop is reduced up to 0.98p.u. And vales the Voltage at dc-link of the DFIGURE (over shoot), and PCC voltage drop also will be reduced with ANFIS. Hence the performance of voltage sag will and swell is improved to 1.7pu.

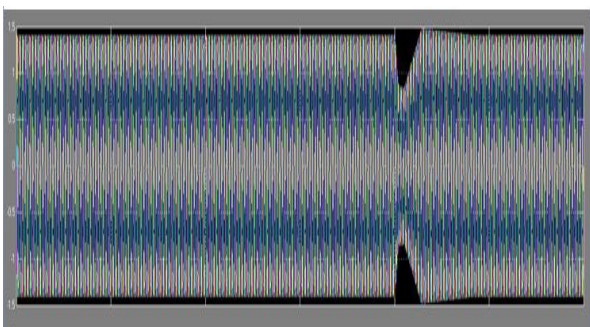


Figure 9: DFIGURE response during Voltage Sag Event without SMES

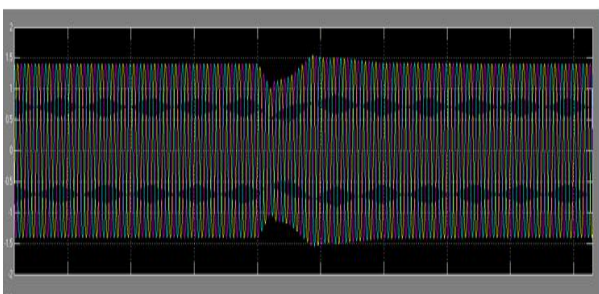


Figure 10: DFIGURE response during Voltage Sag Event with SMES and ANFIS

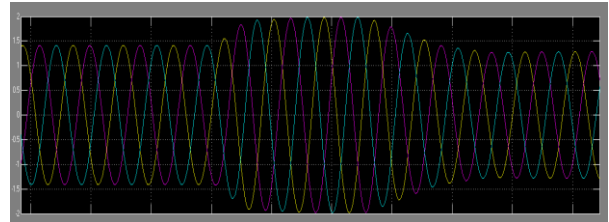


Figure 11: DFIGURE response during Voltage Swell Event without SMES

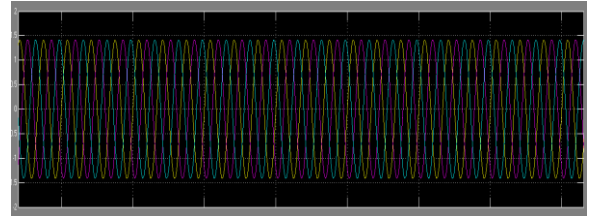


Figure 12: DFIGURE responses during Voltage swell Event with SMES and ANFIS

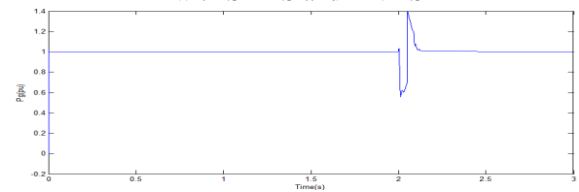


Figure 13 (a): Active power vs time during sag without SMES

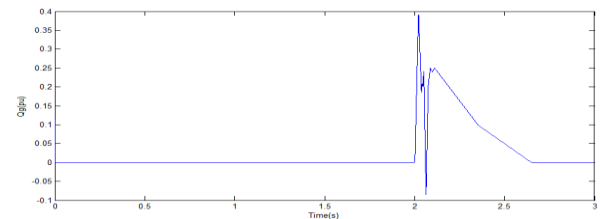


Figure 13 (b): Reactive power vs time during sag without SMES

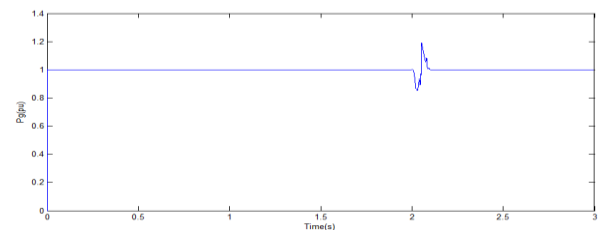


Figure 14 (a): Active power vs time during sag with ANFIS

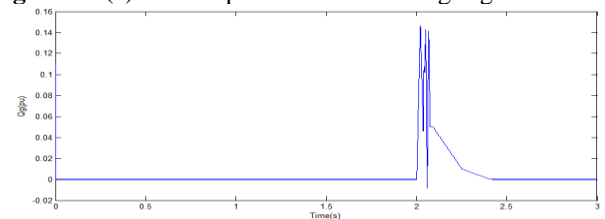


Figure 14 (b): Reactive power vs time during sag with ANFIS

7. Conclusion

A new control algorithm along with a new application of the SMES unit to improve the transient response of WTGs equipped with DFIG during voltage sag and voltage swell events has been proposed. Simulation results have shown that the SMES unit is very effective in improving the dynamic performance of a power system with wind turbine

equipped with DFIGURE during voltage sag and voltage swell at the grid side. The proposed control algorithm of the SMES unit is simple and easy to implement and is able to improve the FRT of the DFIGURE. The SMES unit, on the other hand is still an exorbitant bit of hardware; in any case, because of the improvement of high temperature superconducting materials, its application in power systems is expected to become viable in the near future.

References

- [1] S. Jing, T. Yuejin, X. Yajun, R. Li, and L. Jingdong, "SMES based excitation system for doubly-fed induction generator in wind power application," *IEEE Trans. Appl. Supercond.*, vol. 21, no. 3, pp. 1105–1108, Jun. 2011.
- [2] Dynamic Performance of DFIGURE using SMES For WECS J Srinadh, S Sankara Prasad *PG Student, 2Assistant Professor, EEE Dept., GPCET, INDIA.*
- [3] Superconducting Magnetic Energy Storage System based Improvement of Power Quality on Wind/PV Systems S. Ashwanth1, .Manikandan2, Dr. A. Mahabub Basha.
- [4] F. Beaufays, Y.A. Magid, and B.Windrow, "Application of neural network to load frequency control in power system", *Neural Network*, Vol.7, No.1,pp.183-194,1994.
- [5] S. Hu, X. Lin, Y. Kang, and X. Zou, "An improved low-voltage ride through control strategy of doubly fed induction generator during grid faults," *IEEE Trans. Power Electron.*, vol. 26, no. 12, pp. 3653–3665, Dec. 2011.
- [6] A. Abu-Siada and S. Islam, "Application of SMES unit in improving the performance of an AC/DC power system," *IEEE Trans. Sustainable Energy*, vol. 2, no. 2, pp. 109–121, Apr. 2011.
- [7] A. Abu-Siada, "Application of superconducting magnetic energy storage units to improve power system performance," Ph.D. thesis, Dept. Elect. Eng., Curtin Univ. Technol., Bentley, Australia, 2004.
- [8] M. H. Ali, W. Bin, and R. A. Dougal, "An overview of SMES applications in power and energy systems," *IEEE Trans. Sustainable Energy*, vol. 1, no. 1, pp. 38–47, Apr. 2010.
- [9] H. J. Boenig and J. F. Hauer, "Commissioning tests of the Bonneville power administration 30 MJ superconducting magnetic energy storage unit," *IEEE Trans. Power App. Syst.*, vol. PAS-104, no. 2, pp. 302–312, Feb. 1985.
- [10] M. Altin, O. Goksu, R. Teodorescu, P. Rodriguez, B. B. Jensen, and L. Helle, "Overview of recent grid codes for wind power integration," in *Proc. 12th Int. Conf. OPTIM*, 2010, pp. 1152–1160.
- [11] F. Blaabjerg and Z. Chen, *Power Electronics for Modern Wind Turbines*. Aalborg, Denmark: Morgan & Claypool, 2006, p. 18.
- [12] J. G. Slootweg, S. W. H. de Haan, H. Polinder, and W. L. Kling, "General model for representing variable speed wind turbines in power system dynamics simulations," *IEEE Trans. Power Syst.*, vol. 18, no. 1, pp. 144–151, Feb. 2003.

Author Profile



J. Rajesh student, currently pursuing M. Tech in Power Electronics from Kuppam Engineering College, Kuppam, Chittoor -District, Andhrapradesh, India. Graduated in B.Tech EEE in the year 2009 from S.V. University Tirupathi, Andhra Pradesh.



Dr. Venugopal. N has obtained his doctoral degree from Dr. MGR. University Chennai. B.E. degree and M.E. Degree both from Bangalore University. He has 18 years of teaching experience. His research area is Digital Image Processing, Power Electronics, and Renewable Energy Sources & Video sequence separation. Currently working as an HOD of EEE Department & Director, R & D in Kuppam Engineering College, Kuppam, Chittoor Dist. Andhra Pradesh. His research area of interest includes Power electronics, Renewable Energy Systems and Embedded Systems. He received AICTE & IET grants for research Projects in the areas of Electrical Engineering.